Partitioning the contributions of glacier melt and precipitation to the 1971-2010 runoff increases in a headwater basin of the Tarim River

Zehua Li[1], Xiaogang Shi[2*], Qiuhong Tang[3], Yongqiang Zhang[3], Huilin Gao[4], Xicai Pan[5], Stephen J. Déry[6] and Ping Zhou[1]

[1]*Guangdong Open Laboratory of Geospatial Information Technology and Application, Key Lab of Guangdong for Utilization of Remote Sensing and Geographical Information System, Guangzhou Institute of Geography, Guangzhou, China*
[2]*School of Interdisciplinary Studies, University of Glasgow, Dumfries, UK*
[3]*Key Laboratory of Water Cycle and Related Land Surface Processes, Institute of Geographic Sciences and Natural Resources Research, Chinese Academy of Sciences, Beijing, China*
[4]*Department of Civil Engineering, Texas A & M University, College Station, Texas*
[5]*Institute of Soil Science, Chinese Academy of Sciences, Nanjing, China*
[6]*Environmental Science and Engineering Program, University of Northern British Columbia, Prince George, British Columbia, Canada*

[*]Corresponding author:

Xiaogang Shi (John.Shi@glasgow.ac.uk)

Abstract

Glacier retreat and runoff increases in the last few decades characterize conditions in the Kumalak River Basin, which is a headwater basin of the Tarim River with a catchment area of 12,800 km^2. To address the scientific question of whether, and to what extent, the observed runoff increase can be attributed to enhanced glacier melt and/or increased precipitation, a glacier evolution scheme and precipitation-runoff model are developed. Using the glacio-hydrological model, we find that both glacier cover area and glacier mass in the study area have decreased from 1971 to 2010. On average, the contribution to total runoff from rainfall, glacier melt and snowmelt are 60.6%, 28.2% and 11.2%, respectively. Despite covering only 21.3% of the basin area, glacier areas contributed 43.3% (including rainfall, snowmelt and glacier melt) to the total runoff from our model estimates. Furthermore, as primary causes of increased runoff in response to the warmer and wetter climate over the period 1971-2010, contribution from increases in rainfall and glacier melt are 56.7% and 50.6%, respectively. In comparison to rainfall and glacier melt, snowmelt has a minor influence on runoff increase, accounting for -7.3%. The research has important implications for water resources development in this arid region and for some similar river basins in which glacial melt forms an important part of the hydrological cycle.

Key words: glacio-hydrological modeling, glacier melt, climate change, Tarim River

1 Introduction

Snow cover and glacier ice exert major controls on climate and hydrology over much of the Northern Hemisphere (Barnett et al., 2005). From a climatological perspective, snow and glacier ice interact with the atmosphere over a range of spatial and temporal scales involving complex and sensitive feedback mechanisms (Serreze et al., 2000; Hock, 2005; Déry and Brown, 2007; Shi et al., 2011, 2013; Hock, 2017;). From a hydrological perspective, the contribution of snowmelt and glacier melt to river runoff is of particular interest (Déry et al., 2009; Tang and Lettenmaier, 2010; Kang et al., 2014; Duethmann et al., 2015; Shi et al., 2015; Wang et al., 2015; Yang et al., 2015; Kang et al., 2016; Rupp et al., 2016; Bolch, 2017; Dickerson-Lange et al., 2017). While seasonal snow cover is a more important source of runoff than glacier melt over much of the globe, the latter can be important during at least part of the year for some large river basins (Schaner et al., 2012). Therefore, water managers require knowledge on the implications to water supplies of glacier retreat and potential disappearance as the climate warms (Koboltschnig and Schöner, 2010).

Both ablation and accumulation are sensitive to local and global changes in climate, which are likely to intensify in the coming decades (Gillett et al., 2011; Donat, 2013; Huss and Hock, 2015; Kronenberg et al., 2016). Model studies for the effect of projected changes in air temperature and precipitation on runoff have shown a range of possible outcomes from seasonal shifts in runoff to complete deglaciation in some

43 environments, which can have serious implications for the water supply in terms of
44 affected population and ecosystems (Barnett et al., 2005; Hagg et al., 2006, 2007;
45 Huss et al., 2008). In this paper, we diagnose observed hydrologic changes in a
46 partially glacierized headwater basin in the Tarim River Basin (TRB), shown in
47 Figure 1), which has experienced a positive trend in both air temperature and
48 precipitation over the last few decades. For this basin, we assess changes in glacier
49 area and mass and their relative importance in explaining a positive trend in observed
50 runoff in recent decades.

51 The TRB is one of the world's largest endorheic drainage systems, which is
52 dominated by an arid inland climate (Chen et al., 2006). As the largest inland river in
53 China, the Tarim River spans 1,321 km in length with a drainage area of about 1
54 million km^2. The Aksu, Hotan, Yarkant and Kaidu rivers, which originate in the
55 Tianshan and Kunlun Mountains, feed the main stem of the Tarim River. Amongst
56 these, the Aksu River is the largest tributary, accounting for 70-80% of the Tarim
57 River's discharge observed at Alaer (Figure 1) (Tang et al., 2007; Hao et al., 2015; Li
58 et al., 2016). The runoff in the Aksu basin originates from orographic rainfall,
59 seasonal snowmelt and glacier melt (You, 1995; Jiang et al., 2005). Since the 1980s,
60 the TRB's warm and dry inland climate has experienced increases in both air
61 temperature and precipitation (Shi et al., 2003; 2007; Tao et al., 2011). As a result, the
62 time series from two stream gauges within the Aksu River basin both show a

significant positive trend (Zhang et al., 2010) over the period from 1957 to 2003. In this paper, we address the scientific question of whether, and to what extent, the observed runoff increase can be attributed to enhanced glacier melt and/or increased precipitation. The research has important implications for water resources development in this arid region and for some similar river basins in which glacial melt forms an important part of the hydrological cycle.

Hydrological models provide a way to evaluate the effect of changes in land surface hydrological fluxes and states. Glacio-hydrological models typically consist of two components. The first component determines the amount of melt, while the second part transports the meltwater along the basin. Glacier and snowmelt models range from full energy-balance models that provide a detailed evaluation of surface energy fluxes, to temperature index models in which air temperature acts as a proxy for all terms that are a source of melt energy (Singh, 2001; Hock, 2005). Energy balance melt models more directly describe the physical processes at the glacier surface but require detailed observations, which are often not available, especially in high mountain areas like the Himalayas and Tianshan Mountains. Since air temperature is widely observed, temperature-index methods remain the most widely used approach to compute melt for many purposes. Despite the simplicity, these models often perform remarkably well (Quick and Pipes, 1977; Baker et al., 1982; Tangborn, 1984; Jansson et al., 2003). As a complete set of meteorological data to

drive an energy balance melt model is unavailable for this remote region, we use a temperature index approach in the study.

A key determinant for the evolution of glacier volume and melt in response to climate variations and change is the glacier area distribution with elevation. Aizen et al. (2007) analyzed almost 16,000 glaciers in the Tianshan Mountains and found that the normal distribution can provide a good fit to the empirical histogram of the distribution of Glacier Covered Area (GCA) by altitude for the basins with glacierized areas exceeding 20 km^2. However, the distribution of area with elevation in itself is insufficient to understand the evolution of glaciers over time, something that is of particular interest when examining the effects of variability and change in local climate and their effect on the water balance of glacierized river basins.

In recent years, an increasing number of studies focused on the upper Aksu River Basin by using glacio-hydrological models (Zhao et al., 2013; Duethmann et al., 2015; Wang et al., 2015). Zhao et al. (2013) extended the VIC macroscale land-surface hydrologic model by coupling an energy-balance based glacier scheme for high, cold mountainous regions. In their model, a glacier is described as one special land use/land cover class as well as other vegetation classes. The results in the Aksu River Basin showed obvious improvements in the model performance on runoff simulation. Their results also showed the contribution to runoff from glacier melt was 43.8% in the Kumalak River Basin (called Kunma Like River in their study), and 95.5% of the

increasing runoff was from precipitation runoff. However, this model did not consider glacier mass or glacier area change, and their study did not take observations on glacier mass or glacier area into model calibration/validation, which can lead to wrong estimates of glacier melt and its contribution to runoff. Duethmann et al. (2015) paid more attention to the representation of glacier geometry changes. In the setup of the hydrological model WASA that they used, glacier areas were updated annually by prescribing a constant linear decrease rate during the simulation period. The WASA model was thus well calibrated based on glacier mass balance in addition to discharge data. Their results showed the contribution to runoff from glacier melt was 35-48% in the Kumalak River Basin (called Sari-Djaz catchment in their study), and indicated that both precipitation and temperature had effects on the runoff increase. However, there likely exist inconsistencies between the prescribed constant linear decrease rate and actual change of glacier area, which would lead to inaccuracy in estimating glacier mass balance, glacier melt and its contribution to runoff as well.

To provide a basis for predicting glacier mass and area evolution due to changing temperature and precipitation, we developed a temperature index based model that can simulate the vertical evolution of glacier area and mass at a monthly time step. The major objectives of this study are to use this model to a) simulate catchment glacier and runoff; b) partition the runoff generating mechanisms; and c) determine the possible causes of observed increases in runoff over the last few decades for the

123 headwater basin of the TRB.

124 **2 Study area and datasets**

125 The Kumalak River originates from the Tianshan Mountains and flows through
126 Kyrgyzstan and Kazakhstan before reaching China (Zhao et al., 2013; Wang et al.,
127 2015). With a catchment area of 12,800 km^2, the Kumalak River Basin (KRB)
128 upstream of the hydrometric gauge at Xiehela has a glacier coverage of about 21.3%
129 (Figure 1). The elevation ranges from 1450 m to 7100 m. Monthly mean discharge
130 data for the period of 1971-2010 were obtained from a hydrometric gauge at Xiehela
131 (1450 m). The annual average runoff upstream of Xiehela is 385 mm $year^{-1}$, with a
132 rate of increase of +2.05 mm $year^{-1}$. Compared to the lower reaches of the Aksu River
133 Basin, the upstream area above the gauge is less developed and basically remains in a
134 natural condition during the study period. Monthly maximum and minimum air
135 temperatures, and precipitation from 1971 to 2010 (Figure 2) used to drive the model
136 were derived from the meteorological station at Aksu (1104 m, see Figure 1 for the
137 gauge location), for which quality control is operated by the China Meteorological
138 Administration (CMA). The annual average air temperature observed at Aksu is
139 11.2℃, with a warming rate of ＋0.05℃ $year^{-1}$. The annual average precipitation
140 observed at Aksu is 78.9 mm $year^{-1}$, with a trend of ＋0.55 mm $year^{-1}$.

141

142 Figure 1 inserted here

143 Figure 2 inserted here

144

145 There is a paucity of long-term meteorological observations at higher elevations in
146 the KRB. Therefore, we need to estimate precipitation and air temperature at higher
147 elevations using a seasonal temperature lapse rate and precipitation gradient (Table 1)
148 to adjust model forcings derived from the CMA station at Aksu located within the
149 basin at lower elevations, where precipitation is significantly less than that at higher
150 elevations. The air temperature lapse rate is calculated from data at 242
151 meteorological stations from 1961 to 2007 in western China by distinguishing
152 different altitudes and months (Gao et al., 2010). The precipitation gradient of 0.22
153 mm $year^{-1}$ m^{-1} year in our study is adapted from a study of geostatistics based on the
154 monitoring network maintained by CMA (Jiang et al., 2006; Gao et al., 2010). In
155 Table 2, we summarize a number of observation-based studies with the similar
156 evaluation for orographic precipitation enhancement in this region. The locations of
157 four precipitation gauges used in the previous studies are located in/close to the KRB
158 as shown in Figure 1. All previous studies suggested a significant increase in
159 precipitation with altitudes. This strong orographic gradient is comparable with the
160 results derived from similar observations on the southern slopes of the Tianshan
161 Mountains (Aizen et al., 1997; Zhang et al., 2006; Gao et al., 2008; Li et al., 2012).

162

Table 1 and Table 2 inserted here

The Tianshan Mountains have the largest number of glaciers in northwestern China. A complete set of aerial photographs and large-scale topographic maps covering the glacierized portion of the KRB were collected in the 1970s. The glacier inventory for this region was compiled in 1980. The distribution of glaciers in our research was carefully checked with these maps, aerial photographs and field investigations. In addition, 34 glacier parameters including glacier area, thickness and storage volume were measured and calculated from the maps by Shi et al. (2010).

Kang (1993) found the lapse rate of temperature is larger in the glacierized area than in the non-glacierized area based on measured data. To account for this effect, an amplification coefficient is included as a calibrated parameter based on Zhang et al. (2004) and Gao et al. (2008). The amplification coefficient is applied to the glacierized area as a factor to the original temperature lapse rate. For example, an amplification coefficient of 1.5 means that the temperature lapse rate used in the glacierized area is 50% higher than the original temperature lapse rate input (used in the non-glacierized area). In addition, the calibrated parameters also include a bias factor due to the large uncertainties in areal precipitation (Duethmann et al., 2015). The bias factor is applied to the whole basin as a factor to the original precipitation input, of which 1.5 means that the precipitation used in the model is 50% higher than

the original precipitation input.

3 Model description

We developed a monthly and vertically explicit hydrological model to simulate glacier area and mass evolution as a function of elevation for highly glacierized basins. The model comprises two components. The first component uses a temperature-based method to separate precipitation into rainfall and snowfall, and to estimate snowmelt and glacier melt. The second component routes streamflow from precipitation and melt water at the basin outlet through a Conceptual Rainfall-Runoff (CRR) model Six Parameters (SIXPAR) presented by Gupta and Sorooshian (1983). As a simple model characterized by six parameters, SIXPAR retains some of the important characteristics of the Sacramento Soil Moisture Accounting (SAC-SMA) model, which are described in Section 3.2. Some important equations are listed and described below.

3.1 Glacier and snow mass balance

We used a temperature-based method to separate precipitation into rainfall and snowfall. If monthly minimum temperature (T_{min}) is larger than the threshold temperature (T_{thres} = 0.5℃), then all precipitation is considered as rainfall. If monthly maximum temperature (T_{max}) is lower than the threshold temperature, precipitation is assumed to occur as snowfall. When the threshold temperature is between the minimum and maximum temperatures, the rainfall amount (P_{rain}) is estimated as a

proportion of the total precipitation (P_{total}) as (Leavesley et al., 1983; Gunawardhana and Kazama, 2012):

$$\begin{aligned} P_{rain} &= \frac{T_{\max} - T_{thres}}{T_{\max} - T_{\min}} \times P_{total} \\ P_{snow} &= P_{total} - P_{rain} \end{aligned} \tag{1}$$

As indicated in the above section, the meteorological forcings were corrected by a monthly temperature lapse rate (T_{lapse}) and monthly precipitation gradient (P_{grad}) based on a geostatistical study in the Aksu River Basin (Jiang et al., 2006; Gao et al., 2010). These adjustment factors (Table 1) were applied to each 50-m elevation band, by which the glacial headwater KRB was divided based on a Digital Elevation Model (DEM) of the Shuttle Radar Topography Mission (SRTM) at 1 arc sec resolution (Farr et al., 2007).

Using the degree-day method, the glacier melt and snowmelt processes were assumed to be a function of the sum of the positive air temperatures, with different degree-day factors respectively (Braithwaite, 1995):

$$\begin{cases} M_{glacier} = DDF_{glacier} \sum T^{+} \\ M_{snow} = DDF_{snow} \sum T^{+} \end{cases} \tag{2}$$

$$\sum T^{+} = \begin{cases} 0, & T_{\max} \le T_{thres} \\ \dfrac{(T_{\max} - T_{thres})^2}{2 \cdot (T_{\max} - T_{\min})} \cdot dom, & T_{\min} \le T_{thres} < T_{\max} \\ \dfrac{T_{\max} + T_{\min} - 2 \cdot T_{thres}}{2} \cdot dom, & T_{\min} > T_{thres} \end{cases} \tag{3}$$

where $DDF_{glacier}$ is the degree-day factor for glacier melt and DDF_{snow} is the degree-day factor for snowmelt, and the sum of the positive air temperatures (ΣT^{+})

was estimated based on T_{min}, T_{max} and T_{thres} during each month and days of the month (*dom*). Specifically, glacier melt is defined as the amount of water melt from glacier ice to runoff, whereas snowmelt is defined as the amount of water melt from snowpack to runoff.

The vertical evolution of glacier mass is simulated over the elevation bands in our model. Hence each elevation band as a basic unit of the model, is divided into the glacierized part and non-glacierized part. The glacier area, thickness and storage volume were taken from the Glacier Inventory of China (Shi et al., 2010) and then generated for the year of 1971 as model inputs to initialize and parameterize the glacierized part of each elevation band in our study area. The glacier mass balance is assumed to appear within the glacierized part at each elevation band, where the glacier mass is assumed to be distributed horizontally uniform (same thickness). At each time step, the mass balance of glacier and snow is computed for each elevation band with the thickness updated accordingly. Hence the glacier area and glacier mass with the same elevation band would disappear when melting down. When there is a snowpack on the glacier, the snow melts first before the glacier starts melting. If the accumulated snow at the glacier surface is not completely melted at the end of the ablation season each year, it would turn into ice in the model.

In this research, the model updates the total GCA by summing up the area of glacierzed parts of those elevation bands with glacier ice. Thus the simulated total

GCA is computed at each time step accordingly. Therefore, our model developed in this paper is capable of simulating monthly changes for both glacier and runoff. Based on model simulation results, we calculated the sum of rainfall, snowmelt and glacier melt. Then, the fractions of rainfall, snowmelt and glacier melt were calculated from the sum. Finally, we applied these fractions to the simulated runoff to calculate the corresponding runoff components resulting from rainfall, snowmelt and glacier melt.

3.2 River discharge simulation

The CRR model SIXPAR uses two soil layers to represent the subsurface. The upper zone extends from the surface to the bottom of the root zone, while a lower zone represents ground water storage. The percolation process links the upper and lower zones, simulating the effects of gravity and downward suction (Brazil and Hudlow, 1981). In this study, we employed the modified SIXPAR (Gupta and Sorooshian, 1983) to simulate river discharge. Glacier melt, snowmelt and rainfall form combined inputs to the upper zone (Kite, 1991; Gunawardhana and Kazama, 2012). The Hargreaves equation, which is widely used as an air temperature-based formula, was adopted to estimate potential evapotranspiration (Hargreaves and Samani, 1985). The actual evapotranspiration is calculated based on maximum soil water capacity, actual soil water content and potential evapotranspiration (Zhao, 1992).

4 Methods

4.1 Optimization algorithm

In this study, the Multiobjective Shuffled Complex Evolution Metropolis (MOSCEM-UA) algorithm is used for model calibration (Vrugt et al., 2003). This algorithm is an improvement over the Shuffled Complex Evolution Metropolis (SCEM-UA) global optimization algorithm by using an improved concept of Pareto dominance to evolve the initial population of points toward a set of solutions stemming from a stable distribution (Pareto set) (Shi et al., 2008). The MOSCEM-UA algorithm is used to calibrate ten model parameters (shown in Table 3), including upper and lower zone maximum storage capacities, upper and lower zone recession constants, constants to fit the percolation equation, melt factors for snow and glacier ice, amplification coefficient of temperature lapse rate in glacierized area, and bias factor of precipitation.

4.2 Calibration criteria

Two criteria are used for model calibration to ensure an optimal model performance with respect to both observed discharge and Glacier Mass Balance (GMB). For observed discharge, the first criterion is based on the Nash-Sutcliffe Efficiency (NSE) coefficient (Nash and Sutcliffe, 1970), which is defined as:

$$NSE_Q = 1 - \frac{\sum (Q_{obs} - Q_{sim})^2}{\sum (Q_{obs} - \bar{Q}_{obs})^2} \qquad (-\infty < NSE_Q < 1) \tag{4}$$

with monthly simulated (Q_{sim}) and monthly observed (Q_{obs}) discharge for the calibration period.

By comparing the Digital Terrain Models (DTMs) obtained from 1975 KH-9 Hexagon imagery and the SRTM3 DTM acquired in February 2000, the glacier mass balances were estimated for different regions in the Central Tianshan Mountains (Pieczonka and Bolch, 2015). A region-wide glacier mass loss of -0.35±0.34 m w.e. year^{-1} was observed for the KRB in the period from 1975 to 2000 and is directly used in the calibration for the GMB. Therefore, the second criterion is based on Relative Error (RE), which is applied in the calibration against observed GMB and defined as:

$$RE_{GMB} = \left| \frac{GMB_{sim} - GMB_{obs}}{GMB_{obs}} \right| \quad (5)$$

with the simulated GMB (GMB_{sim}) and the observed GMB (GMB_{obs}) for the calibration period.

We calibrated our model for a 30-year period from 1971 to 2000, using monthly discharge measurements from the Xiehela hydrometric gauge and the observed GMB (Pieczonka and Bolch, 2015). By model calibration, parameters are selected from the Pareto set. The remaining part of the discharge measurements from 2001 to 2010 and the observed change in GCA between 1975 and 2008 (Pieczonka and Bolch, 2015) are used for model validation and evaluation.

4.3 Sensitivity experiments

To identify the effects of temperature and precipitation to the 1971-2010 runoff change, we regenerated two climate scenarios. The first climate scenario is called '1970s temperature', under which the precipitation experiences the natural change but

the temperature is kept at the level of the 1970s. The other climate scenario is called '1970s precipitation', under which the temperature experiences the natural change but the precipitation is kept at the level of the 1970s. The model outputs, such as GCA, glacier mass and runoff, were selected for comparisons from the above two scenarios and the natural climate condition under which the precipitation and temperature experience the natural change.

5 Results

5.1 Model calibration and validation

From the resulting Pareto set, a solution was selected when it has the optimal performance in terms of both monthly discharge and GMB. In Figure 3, the black dot shows the best solution from calibration with NSE_Q = 0.90 and RE_{GMB} = 0.01. The observed and simulated monthly mean runoff during the calibration period from 1971 to 2000 are shown in Figure 4. The simulated GMB during the calibration period is about -0.38 m w.e. year^{-1}. The calibration parameters and their calibrated values are listed in Table 3. The calibrated value of T_{amp} = 1.15 implies the temperature lapse rate in the glacierized area is 15% higher than the temperature lapse rate in the non-glacierized area, indicating that the cooling effect (Kang, 1993) plays an active role in the hydrologic cycle in the glacierized area. In addition, the calibrated value of P_{bias} = 1.00 impies the precipitation bias is not significant in the KRB.

The selected parameter set from calibration was then applied for model

validation when it also has a good performance in term of discharge with NSE_Q = 0.89 during the period from 2001 to 2010. The observed and simulated monthly mean runoff during the validation period from 2001 to 2010 are shown in Figure 4. In addition, the simulated change in GCA approaches -0.15% year^{-1} during the period between 1975 and 2008, in good agreement with the observed value of -0.11% year^{-1} (Pieczonka and Bolch, 2015).

Figure 3 inserted here

Table 3 inserted here

Figure 4 inserted here

As shown in Figure 5(a) and (b), the glacier area and glacier mass under the scenario of '1970s temperature' both experienced a decreasing trend, but with a lower decreasing rate compared to that under the accelerating warming natural climate, implying the temperature in the 1970s was warm enough to promote long lasting glacier melt. While changes in glacier area and glacier mass under the scenario of '1970s precipitation' and natural climate are basically consistent, indicating changes in air temperature largely governed changes in glacier characteristics over the last decades. In comparison, the effect of changes in precipitation is negligible. From Figure 5(c), the effects of air temperature and precipitation changes on runoff are

generally balanced before 2000. After that, the effect of air temperature exceeds the effect of precipitation.

Figure 5 inserted here

5.2 Water balance components

The water balance for the KRB is given by

$$P = E + R + \Delta S \quad (6)$$

where P is the precipitation estimated assuming a seasonal gradient and bias factor, while E denotes actual evapotranspiration and R is runoff, both of which were computed by the model; the residual term ΔS is the water storage change. Positive (negative) ΔS means the water storage of the basin increases (decreases) in the form of soil moisture, snow or glacier ice. Figure 6 shows the monthly mean of each water balance component in Equation (6) from the model simulation (selected solution from calibration) for the period from 1971 to 2010. Figure 6(a) illustrates the seasonal cycle of precipitation (P) from the model simulation, the maximum value of which occurs in July. The annual precipitation averages 643 mm year^{-1}, in which the average rainfall and snowfall are 499 mm year^{-1} and 144 mm year^{-1}, respectively. Figure 6(b) illustrates the seasonal cycle of evapotranspiration (E) from the model simulation, the peak of which occurs in August and the annual evapotranspiration averages 431 mm

year^{-1}. In our model, the simulated fractions of rainfall, snowmelt and glacier melt to the simulated runoff of each month are used to calculate the runoff contribution. Figure 6(c) shows that as the maximum value of runoff from glacier melt occurs in August, with the runoff (R) lagging the precipitation by one month. The annual average runoff is 376 mm year^{-1}, in which rainfall, glacier melt and snowmelt are 228 mm year^{-1} (accounting for 60.6%), 106 mm year^{-1} (accounting for 28.2%) and 42 mm year^{-1} (accouting for 11.2%), respectively. That implies rainfall and glacier melt contribute the majority of the runoff. From Figure 6(d), monthly mean ΔS is negative from July to September, implying the water storage decreases through this period, mainly in the form of evapotranspiration and runoff. Our model results also indicate despite covering only 21.3% of the basin area, the glacier areas contributed 43.3% (including rainfall, snowmelt and glacier melt) to the total runoff in the KRB.

Figure 6 inserted here

5.3 Changes in glacier and runoff

The simulated GCA and glacier mass during the period from 1971 to 2010 are shown respectively in Figure 5(a) and (b). The GCA decreased by a total of 76.3 km^2 during the study period, while the glacier mass declined by a total of 17.9 m w.e. in response to the warming climate with accelerating glacier melt. The largest decrease

of GCA (-14.6 km^2) and of glacier mass (-6.3 m w.e.) appeared concurrently in the 2000s.

Figure 7(a) shows the observed and simulated runoff time series at the Xiehela gauge. Overall, our model depicts accurately the increasing trend in runoff. The increase rate of observed and simulated runoff are +2.05 mm $year^{-1}$ and +1.64 mm $year^{-1}$, respectively. The model simulations, however, cannot reproduce adequately the persistent higher discharge values observed in the 1990s. Insufficient glacier melting due to an incomplete model structure is one possible reason (Shangguan et al., 2017). Other factors such as an underestimation of precipitation due to the sparse gauging network in high elevations are also likely influencing the simulated glacier mass balance and hydrological cycle. Figure 7(b) shows the time series of simulated runoff contribution at the Xiehela gauge during the period from 1971 to 2010. Overall, runoff from rainfall showed an obvious upward trend, with an increase rate of +0.93 mm $year^{-1}$. Concurrently, runoff from snowmelt experienced a slight downward trend, with a decrease rate of -0.12 mm $year^{-1}$. That implies a larger proportion of precipitation shifts to rainfall rather than snowfall as the increasing precipitation occurs with rising temperatures. At the same time, runoff from glacier melt also showed an upward trend, with an increase rate of +0.83 mm $year^{-1}$, in response to the rising temperatures. The contribution to total runoff from rainfall reached the maximum of 61.4% in the 1990s, then dropped to 60.2% in the 2000s. The

contribution to total runoff from glacier melt reached the maximum of 29.9% in the 2000s, 3.0% larger than the minimum value in the 1970s. The contribution to total runoff from snowmelt dropped to the minimum of 9.9% in the 2000s, with 2.2% less than the maximum value in the 1970s. That implies both rainfall and glacier melt are the primary causes of increased runoff in the recent years, while snowmelt has a minor influence in comparison.

Figure 7 inserted here

6 Discussion

During the calibration and validation periods, the model consistently performed well in simulating the changes in glacier and runoff except the observed high flows in the 1990s. This is probably attributed to an underestimation of the precipitation due to the sparse gauging network in high elevations, insufficient glacier melting, and/or other processes such as the rapid release of internal water storage in glaciers (Shangguan et al., 2017). The model performance is considerably lower when looking at annual variations than at monthly series of streamflow. This is because seasonal variations between winter low flow and summer high flow are much more distinct than annual variations.

Our estimates of the contribution to runoff from glacier melt is 28.2% for the

KRB, similar to that of Dikikh (1993) whose estimate is 33%, and lower than those of Zhao et al. (2013) and Duethmann et al. (2015), who derived glacier melt contributions of 43.8% and 35-48%, respectively. Our estimates also indicate the glacier areas contributed 43.3% (including rainfall, snowmelt and glacier melt) to the total runoff, similar to that of Aizen and Aizen (1998) who estimated the contribution of glacier areas was 36-38%. In addition, we concluded both rainfall and glacier melt are the primary causes of increased runoff in recent years, which is similar to the result of Duethmann et al. (2015).

Our estimate for the contribution to runoff from snowmelt is 11.2% in the KRB, lower than that of Zhao et al. (2013) with an estimate of 27.7%. The underestimation is likely due to our assumption for the new snow on the glacier surface, which would turn into ice if it does not melt out at the end of the ablation season. In addition, we do not represent explicitly the densification from snow to ice. Therefore, the temperature index model was used to estimate snowmelt and glacier melt and to update the glacier area and mass at each elevation band. Due to the sparse gauging network in the remote mountainous areas of the TRB, we used a temperature lapse rate and precipitation gradient to adjust model forcings based on low elevation observing stations to reflect the elevation dependence of air temperature and precipitation. This could lead to uncertainties in our modeling results especially at higher elevations where the glacio-hydrologic process is the most dynamic. Better observations in these

areas would reduce these uncertainties.

A number of previous studies have quantified the role of glacier melt and precipitation increases in runoff increase by using hydrological simulation approach. Zhao et al. (2013) found that runoff increase over the period of 1970-2007 was 96% due to precipitation increase and 4% due to glacier melt increase. However, Duethmann et al. (2015) estimated that temperature increase was the dominant driver to runoff increase over the period of 1957-2004. In contrast, our study provided an estimate for both rainfall and glacier melt that are the primary causes of increased runoff in the study area over the period of 1971-2010. Except that the analyzed time periods of those studies were not completely overlapped, the main difference among these studies lie in the model parameterizations and calibrations, which would result in considerable uncertainties. Furthurmore, most of those models could simulate the glacier mass evolution but without including an explicit representation of glacier flow. The increased ablation at low elevations and enhanced accumulation at high elevations would lead to a steepening of glacier surface, a corresponding increase in driving stress and accelerating ice flow. These effects are likely important for determining glacier mass redistribution over the past years. Therefore, it is worthwhile to put more attention in the design of future observation networks, as well as modeling and prediction work.

7 Conclusions

Using a glacio-hydrological model, we investigated the water balance dynamics of a highly glacierized basin in the TRB, which has experienced increases in both air temperature and precipitation during the last few decades. Our key findings are: a) the contribution to total runoff from rainfall, glacier melt and snowmelt are 60.6%, 28.2% and 11.2%, respectively on average over the period from 1971 to 2010; b) the glacier areas contributed 43.3% (including rainfall, snowmelt and glacier melt) to the total runoff; c) as the primary causes of increased runoff (increase rate of 1.64 mm $year^{-1}$) in response to the warmer and wetter climate over the period of 1971-2010, the contribution from rainfall and glacier melt increase are +0.93 mm $year^{-1}$ and +0.83 mm $year^{-1}$, accounting for 56.7% and 50.6%, while conbritution from snowmelt increase is -0.12 mm $year^{-1}$, accouting for -7.3%.

Acknowledgments

The authors are grateful to Professor Dennis P. Lettenmaier at the University of California, Los Angeles, and Professor Bart Nijssen at the University of Washington for their guidance and help. The work was financially supported by the Guangdong Provincial Science and Technology Program (2018B030324001), GDAS' Special Project of Science and Development (2019GDASYL-0104001, 2019GDASYL-0401001, 2020GDASYL-20200103002), and partially supported by the University of Glasgow CoSS strategic Research Fund, the Strategic Priority Research Program of Chinese Academy of Sciences (XDA20060402) and NSFC

480 (31770493, 41790424, 41730645). We thank two anonymous reviewers for their
481 thorough and constructive reviews.

References

Aizen, V.B., Aizen, E.M., Dozier, J., Melack, J.M., Sexton, D.D., Nesterov, V.N., 1997. Glacial regime of the highest Tien Shan mountain, Pobeda-Khan Tengry massif. Journal of Glaciology 43(145), 503-512.

Aizen, V.B., Aizen, E.M., 1998. Estimation of glacial runoff to the Tarim River, Central Tien Shan. IAHS-AISH Publication 248, 191-198.

Aizen, V. B., 1998. The glaciations and its evolution in the North Tien Shan. PhD Thesis, Moscow, USSR Academy of Science 210. (in Russian)

Aizen, V. B., Aizen, E.M., and Kuzmichonok, V.A., 2007. Glaciers and hydrological changes in the Tien Shan: simulation and prediction. Environmental Research Letters 2, 45019.

Baker, D., Escher-Vetter, H., Oerter, H., Reinwarth, O., 1982. A glacier discharge model based on results from field studies of energy balance, water storage and flow. Hydrological Aspects of Alpine and High-Mountain Areas(138), 103.

Barnett, T.P., Adam, J.C., Lettenmaier, D.P., 2005. Potential impacts of a warming climate on water availability in snow-dominated regions. Nature 438(7066), 303-309, DOI: 10.1038/nature04141.

Bolch, T., 2017. Hydrology: Asian glaciers are a reliable water source. Nature 545(7653), 161.

Braithwaite, R. J., 1995. Positive degree-day factors for ablation on the Greenland ice

502 sheet studied by energy-balance modeling. Journal of Glaciology 41(137), 153-160.
503 Brazil, L.E., Hudlow, M.D., 1981. Calibration procedures used with the National
504 Weather Service river forecast system, Pergamon.
505 Burnash, R.J.C., and Ferral, R.L., 1974. A generalized streamflow simulation system.
506 Mathematical Models in Hydrology, 2.
507 Chen, Y., Takeuchi, K., Xu, C., Chen, Y., Xu, Z., 2006. Regional climate change and
508 its effects on river runoff in the Tarim Basin, China. Hydrological Processes 20(10),
509 2207-2216, DOI: 10.1002/hyp.6200.
510 Déry, S.J., Brown, R.D., 2007. Recent Northern Hemisphere snow cover extent trends
511 and implications for the snow-albedo feedback. Geophysical Research Letters 34,
512 L22504, DOI: 10.1029/2007GL031474.
513 Déry, S.J., Stahl, K., Moore, R.D., Whitfield, P.H., Menounos, B., Burford,
514 J.E., 2009. Detection of runoff timing changes in pluvial, nival, and glacial rivers of
515 western Canada. Water Resources Research 45, W04426, DOI:
516 10.1029/2008WR006975.
517 Dickerson-Lange, S.E., Gersonde, R. F., Hubbart, J.A., Link, T.E., Nolin, A.W., Perry,
518 G.H., Roth, T.R., Wayand, N.E., Lundquist, J.D., 2017. Snow disappearance timing is
519 dominated by forest effects on snow accumulation in warm winter climates of the
520 Pacific Northwest, United State. Hydrological Processes 31(10).
521 Dikikh, A.N., 1993. Lednikovyi stok rek Tyan-Shanya i ego rol' v formirovanii

522 obshego stoka [Glacier runoff in the rivers of Tien Shan and its role in total runoff
523 formation]. Materialy Glaciologicheskikh Issledovanii 77, 41-50.
524 Donat, M.G., 2013. Projection and prediction: Local noise and global confidence.
525 Nature Climate Change 3(12), 1018-1019，DOI: 10.1038/nclimate2061.
526 Duethmann, D., Bolch, T., Farinotti, D., Kriegel, D., Vorogushyn, S., Merz, B.,
527 Pieczonka, T., Jiang, T., Su, B., Güntner, A., 2015. Attribution of streamflow trends
528 in snow and glacier melt-dominated catchments of the Tarim River, Central Asia.
529 Water Resources Research 51, 4727-4750, DOI:10.1002/2014WR016716.
530 Farr, T., Rosen, P., Caro, E., Crippen, R., Duren, R., Hensley, S., Kobrick, M., Paller,
531 M., Rodriguez, E., Roth, L., Seal, D., Shaffer, S., Shimada, J., Umland, J., Werner, M.,
532 Oskin, M., Burbank, D., Alsdorf, D., 2007. The Shuttle Radar Topography Mission.
533 Reviews of Geophysics, 45(2), RG2004.
534 Gao, Q., Wang, R., Giese, E., 2008. Impact of climate change on surface runoff of
535 Tarim River originating from the south slopes of the Tianshan Mountains. Journal of
536 Glaciology and Geocryology 30(1), 1-11. (in Chinese)
537 Gao, X., Ye, B., Zhang, S., Qiao, C., Zhang, X., 2010. Glacier runoff variation and its
538 influence on river runoff during 1961–2006 in the Tarim River Basin, China. Science
539 China Earth Sciences 53(6), 880-891,
540 DOI: 10.1007/s11430-010-0073-4.
541 Gillett, N.P., Arora, V.K., Zickfeld, K., Marshall, S.J., Merryfield, W.J., 2011.

542 Ongoing climate change following a complete cessation of carbon dioxide emissions.
543 Nature Geoscience 4(2), 83-87, DOI: 10.1038/ngeo1047.
544 Gunawardhana, L.N., Kazama, S., 2012. A water availability and low-flow analysis of
545 the Tagliamento River discharge in Italy under changing climate conditions.
546 Hydrology and Earth System Sciences 16(3), 1033-1045,
547 DOI: 10.5194/hess-16-1033-2012.
548 Hagg, W., Braun, L., Weber, M., Becht, M., 2006. Runoff modelling in glacierized
549 Central Asian catchments for present-day and future climate. Nordic Hydrology
550 37(2), 93-105, DOI: 10.2166/nh.2006.001.
551 Hagg, W., Braun, L., Kuhn, M., Nesgaard, T., 2007. Modelling of hydrological
552 response to climate change in glacierized Central Asian catchments. Journal of
553 Hydrology 332(1), 40-53, DOI: 10.1016/j.jhydrol.2006.06.021.
554 Gao, Q., Wang, R., Giese, E., 2008. Impact of climate change on surface runoff of
555 Tarim River originating from the south slopes of the Tianshan mountains. Journal of
556 Glaciology and Geocryology 30(1), 1-11. (in Chinese)
557 Gupta, V. K., Sorooshian, S., 1983. Uniqueness and observability of conceptual
558 rainfall-runoff model parameters: The percolation process examined. Water
559 Resources Research 19(1), 269–276, DOI: 10.1029/WR019i001p00269.
560 Hao, Z., Chen, S., Li, Z., Yu, Z., Shao, Q., Yuan, F., Shi, F., 2015. Quantitative
561 assessment of the impacts of irrigation on surface water fluxes in the Tarim River,

562 China. Hydrology Research 46(6), 996-1007,
563 DOI: http://dx.doi.org/10.2166/nh.2015.215.
564 Hargreaves, G.H., Samani, Z.A., 1985. Reference crop evapotranspiration from
565 ambient air temperature. American Society of Agricultural Engineers.
566 Hock, R., 2003. Temperature index melt modelling in mountain areas. Journal of
567 Hydrology 282(1), 104-115, DOI: 1016/S0022-1694(03)00257-9.
568 Hock, R., 2005. Glacier melt: A review of processes and their modeling. Progress in
569 Physical Geography 29(3), 362, DOI: 10.1191/0309133305pp453ra.
570 Hock, R., Hutchings, J.K., Lehning, M., 2017. Grand challenges in cryospheric
571 sciences: toward better predictability of glaciers, snow and sea ice. Frontiers in Earth
572 Science 5, 64.
573 Huss, M., Farinotti, D., Bauder, A., Funk, M., 2008. Modelling runoff from highly
574 glacierized alpine drainage basins in a changing climate. Hydrological Processes
575 22(19), 3888-3902, DOI: 10.1002/hyp.7055.
576 Huss, M., Hock, R., 2015. A new model for global glacier change and sea-level rise.
577 Frontiers in Earth Science 3, 54, DOI: 10.3389/feart.2015.00054.
578 Jansson, P., Hock, R., Schneider, T., 2003. The concept of glacier storage: a review.
579 Journal of Hydrology 282(1), 116-129,
580 DOI: 10.1016/S0022-1694(03)00258-0.
581 Jiang, Y., Zhou, C., Cheng, W., 2005. Analysis on Runoff Supply and Variation

582 Characteristics of Aksu Drainage Basin. Journal of Natural Resources 20(1), 27-34.
583 (in Chinese)
584 Jiang, Y., Zhou, C., Cheng, W., 2006. Research on the spatial variability of rainfall in
585 Akesu River Basin. Geo-Information Science 8, 131-138. (in Chinese)
586 Kang, D.H., Shi, X., Gao, H., Déry, S.J., 2014. On the changing contribution of snow
587 to the hydrology of the Fraser River Basin, Canada, Journal of Hydrometeorology 15,
588 1344-1365.
589 Kang, D.H., Gao, H., Shi, X., Islam, S., Déry, S.J., 2016. Impacts of a rapidly
590 declining mountain snowpack on streamflow timing in Canada's Fraser River Basin,
591 Scientific Reports 6, 19299, DOI: 10.1038/srep19299.
592 Kang, X., 1993. Temperature and its characteristics in glaciation area. Acta
593 Geographica Sinica 48(2), 152-160. (in Chinese)
594 Kite, G.W., 1991. A watershed model using satellite data applied to a mountain basin
595 in Canada. Journal of Hydrology 128(1-4), 157-169,
596 DOI: 10.1016/0022-1694(91)90136-6.
597 Koboltschnig, G.R., Schöner, W., 2011. The relevance of glacier melt in the water
598 cycle of the Alps: the example from Austria. Hydrology and Earth System Sciences
599 15(6), 2039-2048, DOI: 10.5194/hess-15-2039-2011.
600 Kronenberg, M., Barandun, M., Hoelzle, M., Huss, M., Farinotti, D., Azisov, E.,
601 Usubaliev, R., Gafurov, A., Petrakov, D. KÄÄB, A., 2016. Mass-balance

602 reconstruction for Glacier No. 354, Tien Shan, from 2003 to 2014. Annals of
603 Glaciology 57(71): 92-102, DOI: 10.3189/2016AoG71A032.
604 Leavesley, G.H., Troutman, B.M., Saindon, L.G. (1983), Precipitation-runoff
605 modeling system: User's manual, US Geological Survey.
606 Li, J., Liu, S., Han, H., Zhang, Y., Wang, J., Wei, J., 2012. Evaluation of runoff from
607 Koxkar Glacier Basin, Tianshan Mountains, China. Advances in Climate Change
608 Research 8(5), 350-356. (in Chinese)
609 Li, Z., Hao, Z., Shi, X., Déry, S.J., Li, J., Chen, S., Li, Y., 2016. An agricultural
610 drought index to incorporate the irrigation process and reservoir operations: a case
611 study in the Tarim River Basin. Global and Planetary Change 143, 10-20, DOI:
612 10.1016/j.gloplacha.2016.05.008
613 Nash, J., Sutcliffe, J.V., 1970. River flow forecasting through conceptual models part
614 I - A discussion of principles. Journal of Hydrology 10(3), 282-290, DOI:
615 10.1016/0022-1694(70)90255-6.
616 Osmonov, A., Bolch, T., Xi, C., Kurban, A., Guo, W., 2013. Glacier characteristics
617 and changes in the Sary-Jaz River Basin (Central Tien Shan, Kyrgyzstan) –
618 1990-2010. Remote Sensing Letters 4(8), 725-734, DOI:
619 10.1080/2150704X.2013.789146.
620 Peck, E.L., 1976. Catchment modeling and initial parameter estimation for the
621 National Weather Service River Forecast System, Office of Hydrology, National

622 Weather Service.

623 Pieczonka, T., Bolch, T., 2015. Region-wide glacier mass budgets and area changes
624 for the central Tien Shan between ~1975 and 1999 using hexagon kh-9
625 imagery. Global and Planetary Change 128, 1-13.

626 Quick, M., Pipes, A., 1977. UBC Watershed Model. Hydrological Sciences Journal
627 22(1), 153-161, DOI: 10.1080/02626667709491701.

628 Rupp, D.E., Abatzoglou, J.T., Mote, P.W., 2016. Projections of 21st century climate
629 of the Columbia River Basin. Climate Dynamics 49(5-6), 1-17.

630 Schaner, N., Voisin, N., Nijssen, B., Lettenmaier, D.P., 2012. The contribution of
631 glacier melt to streamflow. Environmental Research Letters 7(3), 034029, DOI:
632 10.1088/1748-9326/7/3/034029.

633 Serreze, M.C., Walsh, J.E., Chapin III, F.S., Osterkamp, T., Dyurgerov, M.,
634 Romanovsky, V., Oechel, W.C., Morison, J., Zhang, T., Barry, R.G., 2000.
635 Observational evidence of recent change in the northern high-latitude environment.
636 Climatic Change 46, 159–207.

637 Shangguan, D., Ding, Y., Liu, S., Xie, Z., Pieczonka, T., Xu, J., Moldobekov, B.,
638 2017. Quick release of internal water storage in a glacier leads to underestimation of
639 the hazard potential of glacial lake outburst floods from Lake Merzbacker in central
640 Tian shan Mountains. Geophysical Research Letters 44(19), 2017GL074443.

641 Shen, Y., Wang, G., Ding, Y., Mao, W., Liu, S., Wang, S., Duishen, M.M., 2009.

642 Changes in glacier mass balance in watershed of Sary Jaz-Kumarik Rivers of
643 Tianshan Mountains in 1957-2006 and their impact on water resources and trend to
644 end of the 21th century. Journal of Glaciology and Geocryology 31(5), 792-800. (in
645 Chinese)
646 Shi, X., Wood, A., Lettenmaier, D.P., 2008. How essential is hydrologic model
647 calibration to seasonal streamflow forecasting? Journal of Hydrometeorology 9(6),
648 1350-1363, DOI: 10.1175/2008JHM1001.1.
649 Shi, X., Groisman, P.Y., Déry, S.J., Lettenmaier, D.P., 2011. The role of surface
650 energy fluxes in pan-arctic snow cover changes. Environmental Research Letters 6(3),
651 035204, DOI: 10.1088/1748-9326/6/3/035204.
652 Shi, X., Déry, S.J., Groisman, P.Y., Lettenmaier, D.P., 2013. Relationships between
653 recent pan-arctic snow cover and hydroclimate trends. Journal of Climate 26(6),
654 2048-2064.
655 Shi, X., Marsh, P., Yang, D., 2015. Warming spring air temperatures, but delayed
656 spring streamflow in an Arctic headwater basin. Environmental Research Letters 10,
657 064003.
658 Shi, Y., Shen, Y., Li, D., Zhang, G., Ding, Y., Hu, R., Kang, E., 2003. Discussion on
659 the present climate change from warm-dry to warm-wet in Northwest China.
660 Quaternary Sciences 23(2), 152-164. (in Chinese)
661 Shi, Y., Shen, Y., Kang, E., Li, D., Ding, Y., Zhang, G., Hu, R., 2007. Recent and

662 future climate change in northwest China. Climatic Change 80(3), 379-393, DOI:
663 10.1007/s10584-006-9121-7.
664 Shi, Y., Liu, C., Kang, E., 2010. The Glacier Inventory of China. Annals of
665 Glaciology 50(53), 1-4, DOI: http://dx.doi.org/10.3189/172756410790595831.
666 Singh, P., 2001. Snow and glacier hydrology, Springer.
667 Sorooshian, S., 1983. Uniqueness and Observability of Conceptual Rainfall-Runoff
668 Model. Water Resources Research 19(1), 269-276,
669 DOI: 10.1029/WR019i001p00629.
670 Tang, Q., Hu, H., Oki, T., 2007. Groundwater recharge and discharge in a hyperarid
671 alluvial plain (Akesu, Taklimakan Desert, China). Hydrological Processes 21,
672 1345-1353, doi: 10.1002/hyp.6307.
673 Tang, Q., Lettenmaier, D.P., 2010. Use of satellite snow-cover data for streamflow
674 prediction in the Feather River Basin, California. International Journal of Remote
675 Sensing 31, 3745-3762, DOI: 10.1080/01431161.2010.483493.
676 Tangborn, W.V., 1984. Prediction of glacier derived runoff for hydroelectric
677 development. Geografiska Annaler. Series A. Physical Geography 257-265.
678 Tao, H., Gemmer, M., Bai, Y., Su, B., Mao, W., 2011. Trends of streamflow in the
679 Tarim River Basin during the past 50 years: Human impact or climate change?.
680 Journal of Hydrology 400(1-2), 1-9.
681 Vrugt, J.A., Gupta, H.V., Bastidas, L.A., Bouten, W., Sorooshian, S., 2003. Effective

682 and efficient algorithm for multiobjective optimization of hydrologic models. Water
683 Resources Research 39(8), 1214, DOI: 10.1029/2002WR001746.
684 Wang, X., Luo, Y., Sun, L., Zhang, Y., 2015. Assessing the effects of precipitation
685 and temperature changes on hydrological processes in a glacier-dominated catchment.
686 Hydrological Processes 29, 4830-4845, DOI: 10.1002/hyp.10538.
687 Yang, D., Shi, X., Marsh, P., 2015. Variability and extreme of Mackenzie River daily
688 discharge during 1973-2011, Quaternary International 380-381, 159-168.
689 You, P., 1995. Surface Water Resources and Runoff Composition in the Tarim River
690 Basin. Arid Land Geography 18(2), 29-35. (in Chinese)
691 Zhang, Y., Liu, S., Han, H., 2004. Characteristics of Climate on the Keqicar Glacier
692 on the South Slopes of the Tianshan Mountains during Ablation Period. Journal of
693 Glaciology and Geocryology 26(5), 545-550. (in Chinese)
694 Zhang, Y., Liu, S., Ding, Y., Li, J., Shangguan, D., 2006. Preliminary study of mass
695 balance on the Keqicar Baxi Glacier on the south slopes of Tianshan Mountains.
696 Journal of Glaciology and Geocryology 28(4), 477-484. (in Chinese)
697 Zhang, Q., Xu, C., Tao, H., Jiang, T., Chen, Y., 2010. Climate changes and their
698 impacts on water resources in the arid regions: a case study of the Tarim River basin,
699 China. Stochastic Environmental Research and Risk Assessment 24(3), 349-358,
700 DOI: 10.1007/s00477-009-0324-0.
701 Zhao, Q., Ye, B., Ding, Y., Zhang, S., Yi, S., Wang, J., Shangguan, D., Zhao, C., Han,

H., 2013. Coupling a glacier melt model to the variable infiltration capacity (VIC) model for hydrological modeling in north-western China, Environmental Earth Sciences 68(1), 87-101.

Zhao, R., 1992. The Xinanjiang model applied in China. Journal of Hydrology 135(1-4), 371-381.

Figures

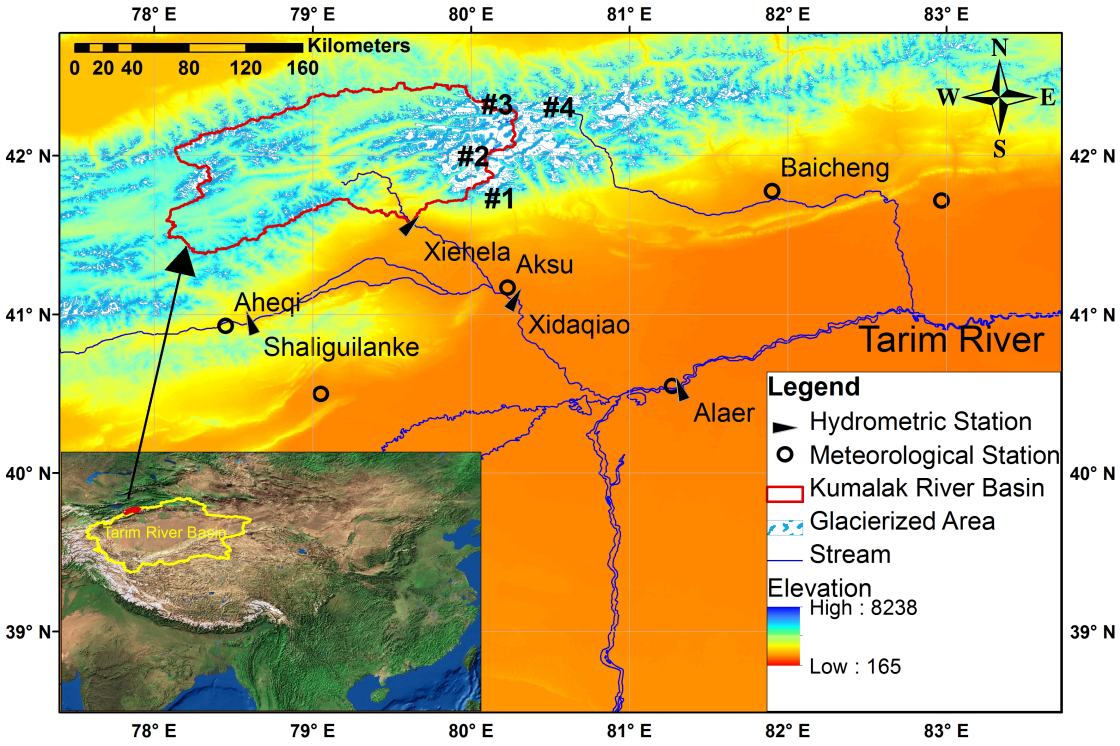

Figure 1 Location of study area (#1, #2, #3 and #4 indicate the locations of observation-based studies referred by Table 1).

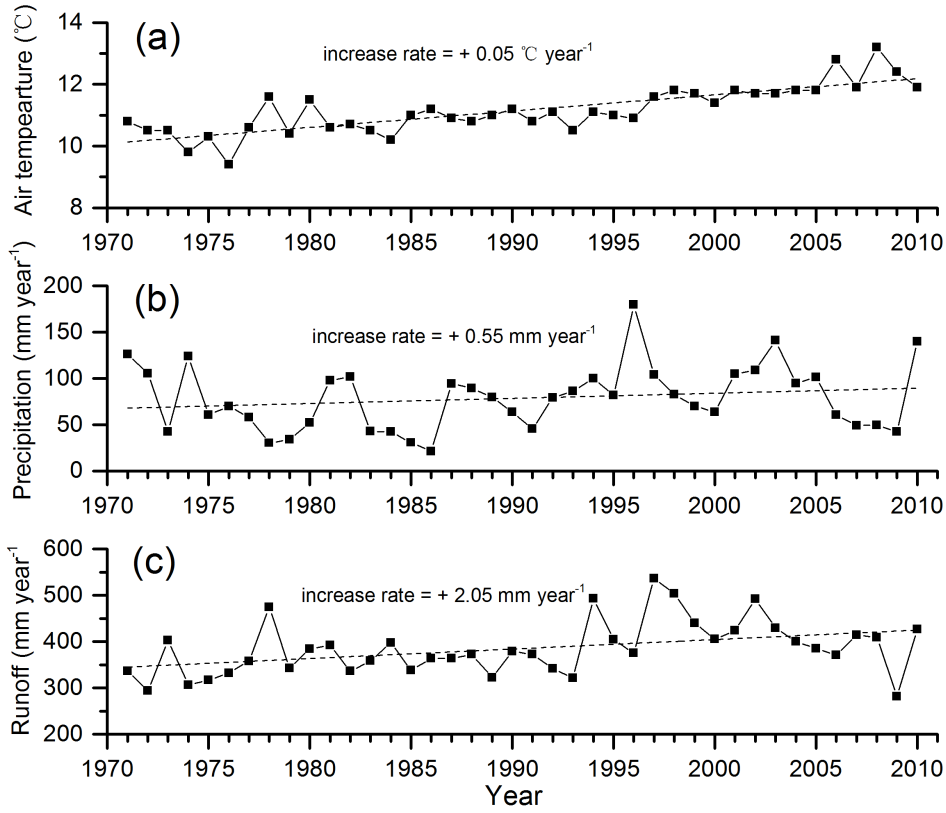

Figure 2 Annual average air temperature and precipitation at Aksu and runoff at the Xiehela gauging station during 1971-2010 with trend slopes.

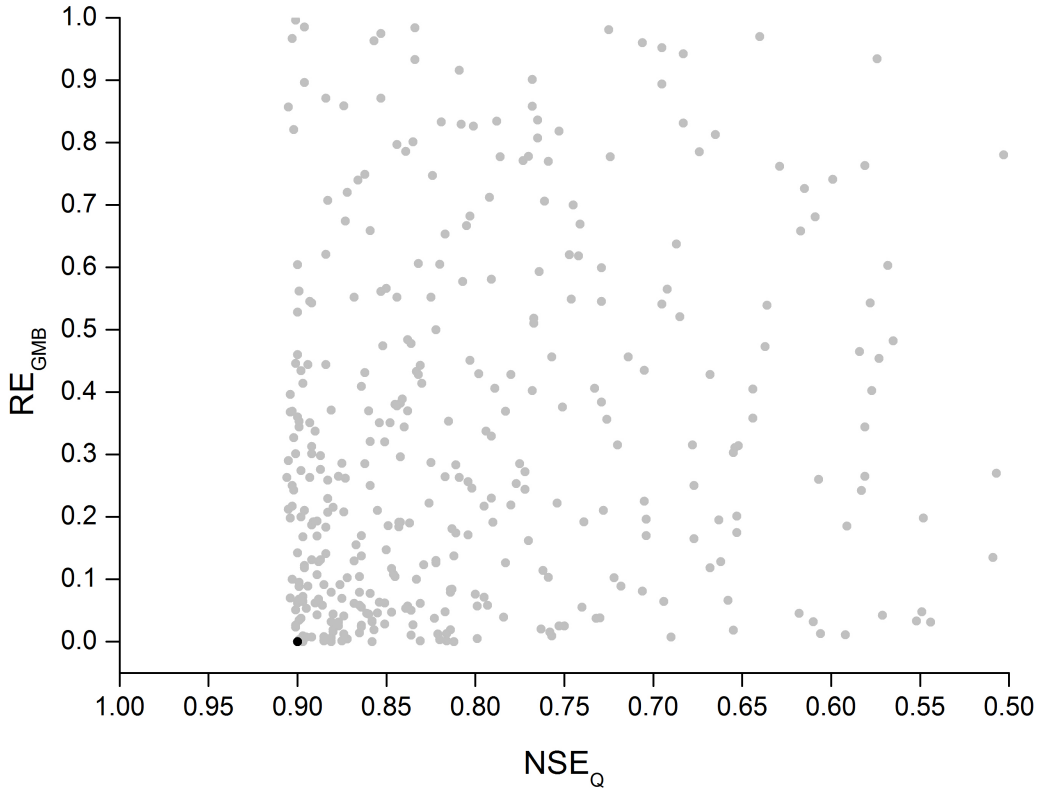

Figure 3 Model performance with respect to observed monthly mean discharge (NSE_Q) against model performance with respect to observed GMB (RE_{GMB}). Solution is selected from calibration and used for further analyses (black dot).

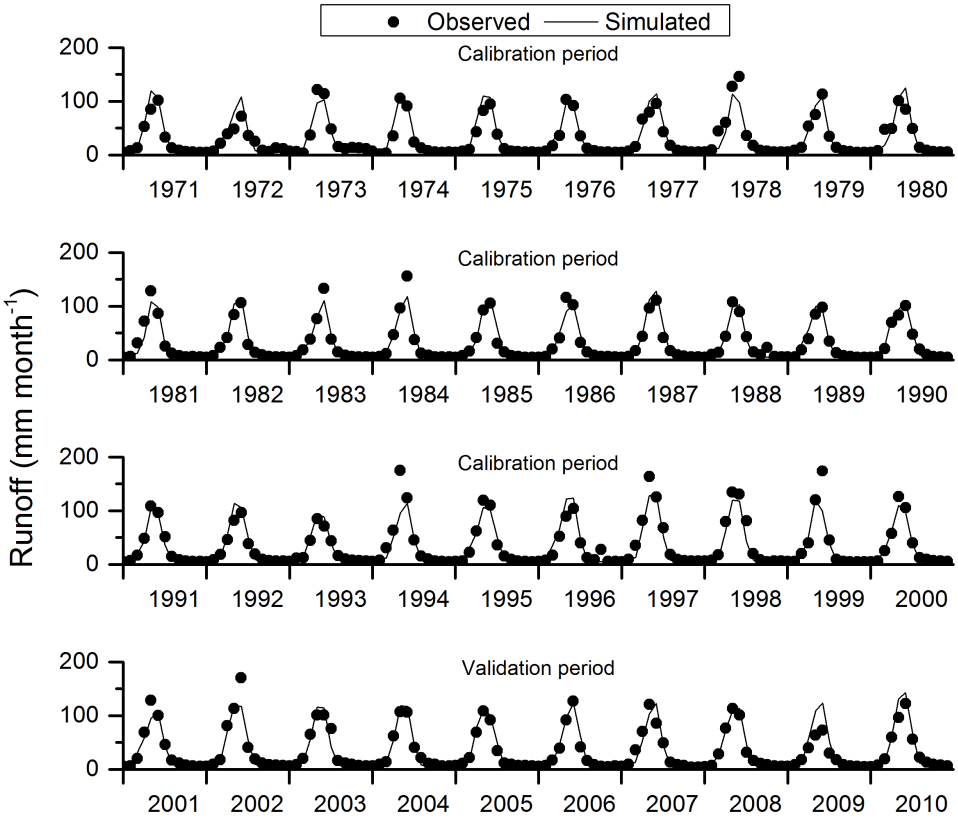

Figure 4 Observed and simulated monthly mean runoff during the calibration period from 1971 to 2000 and the validation period from 2001 to 2010.

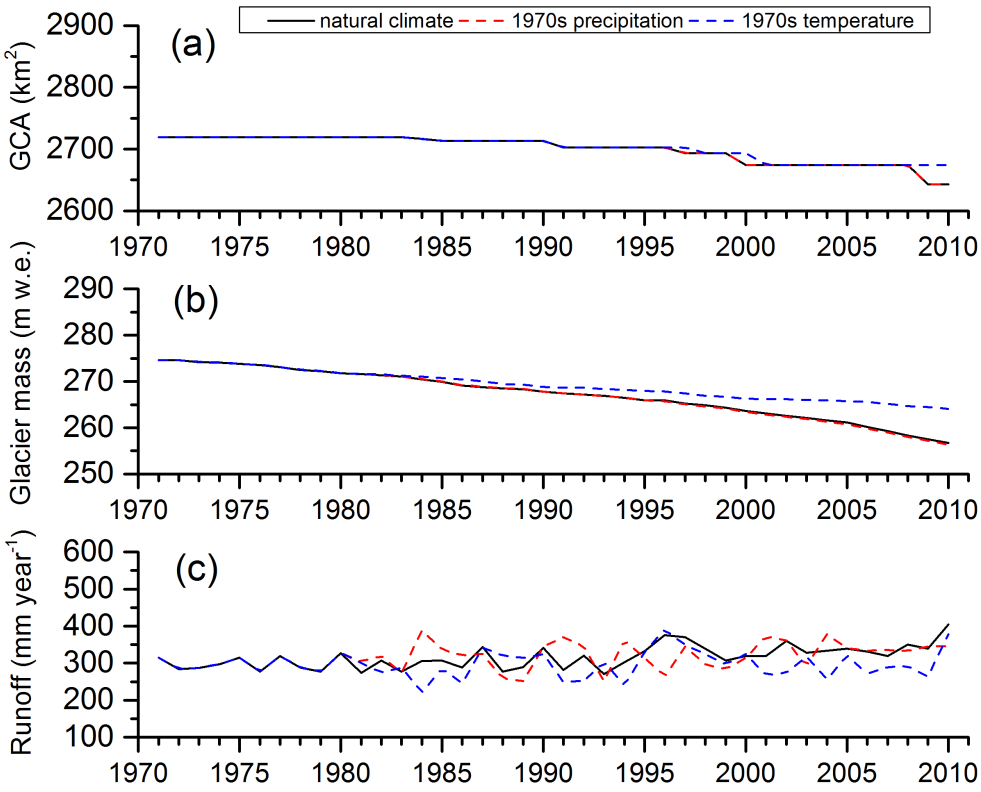

Figure 5 (a) Simulated Glacier Covered Area (GCA); (b) Simulated glacier mass; (c) Simulated runoff under the natural climate, 1970s temperature and 1970s precipitation scenarios during the period from 1971 to 2010.

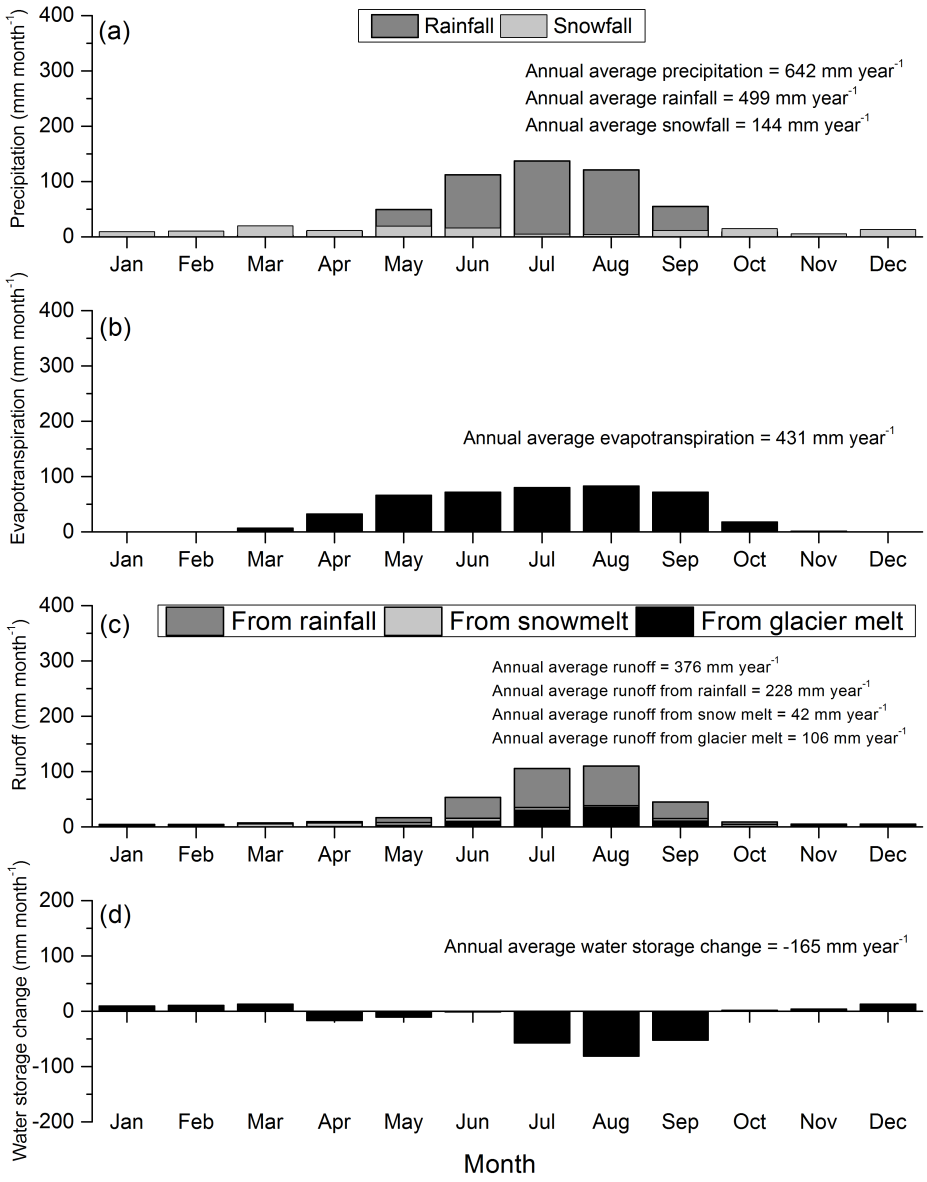

Figure 6 1971-2010 mean monthly climatology of (a) Precipitation (*P*); (b) Evapotranspiration (*E*); (c) Runoff (*R*) from rainfall, snowmelt and glacier melt; (d) Water storage change (*ΔS*).

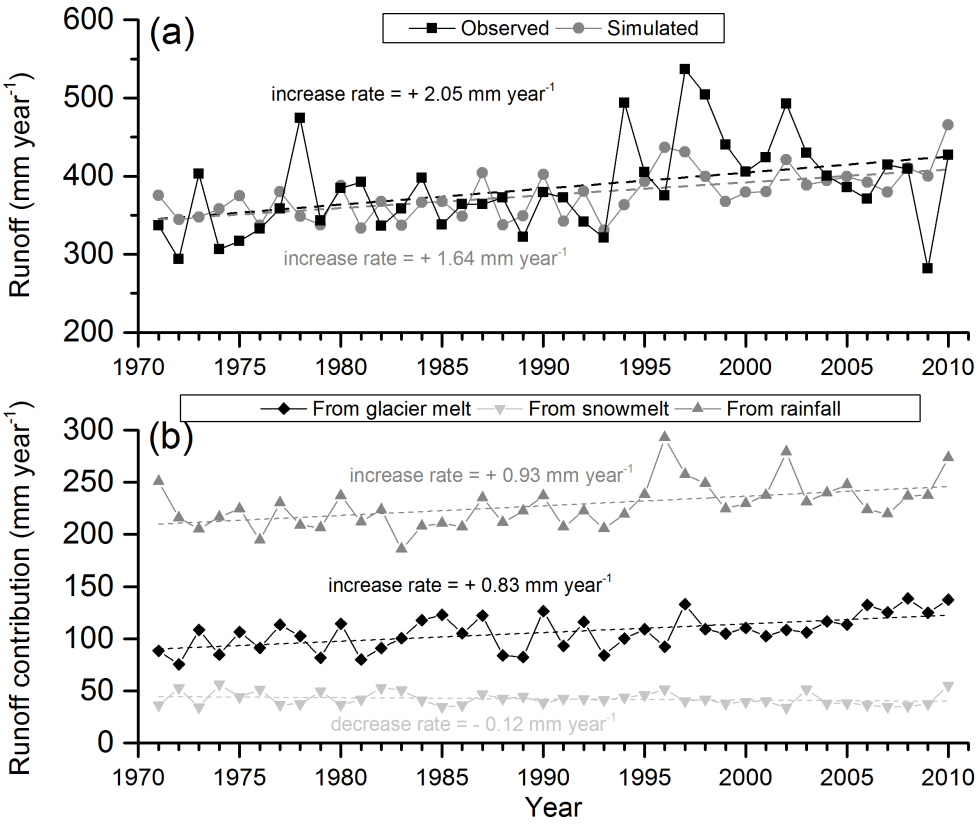

Figure 7 (a) Observed and simulated runoff with trend slopes; (b) Simulated runoff contribution from glacier melt, snowmelt and rainfall with trend slopes during the period from 1971 to 2010.

Tables

Table 1 Monthly air temperature lapse rate (T_{lapse}) and precipitation gradient (P_{grad}) in the Kumalak River Basin.

Month	Jan	Feb	Mar	Apr	May	Jun	Jul	Aug	Sep	Oct	Nov	Dec
T_{lapse} (℃ (100m)$^{-1}$)	0.29	0.39	0.48	0.58	0.61	0.63	0.59	0.56	0.53	0.47	0.43	0.31
P_{grad} (mm (100m)$^{-1}$)	0.29	0.35	0.75	0.75	2.33	4.59	4.81	4.35	2.37	0.77	0.20	0.42

Table 2 The vertical change of precipitation in Central Tianshan.

Annual Average Precipitation (mm)	Altitude (m)	Period	Source	Location
652	3020	2003-2005	(Zhang et al., 2006)	Observations at Keqicar Baxi Glacier (#1)
669 566 830	3000 3700 4200	2004-2010	(Li et al., 2012)	Observations at Koxkar Glacier (#2)
233 600 810	2334 4000 5000	1980s	(Gao et al., 2008)	Estimates based on glacier expedition at the south slopes of the Tianshan Mountains (#3)
>900	6100	Long term	(Aizen et al., 1997)	Observations and glacier expedition at Inylchek Glacier (#4)

Table 3 Model parameters with values and units.

Parameter	Symbol	Value	Units
Upper zone maximum storage capacity	UM	31.0	mm
Lower zone maximum storage capacity	LM	87.5	mm
Upper zone recession constant	UK	0.44	-
Lower zone recession constant	LK	0.07	-
Constants to fit the percolation equation	A	0.22	-
	X	23.3	-
Melt factor for snow	DDF_{snow}	1.48	mm day^{-1} ℃$^{-1}$
Melt factor for glacier ice	$DDF_{glacier}$	3.09	mm day^{-1} ℃$^{-1}$
Amplificaton coefficient of temperature lapse rate in glacierized area	T_{amp}	1.15	-
Bias factor of precipitation	P_{bias}	1.00	-